European Journal of Mechanics B/Fluids 28 (2009) 558–563

Contents lists available at ScienceDirect

European Journal of Mechanics B/Fluids

www.elsevier.com/locate/ejmflu

Free surface deformation due to a source and a sink of equal strength in Stokes flow

Jae-Tack Jeong

School of Mechanical Systems Engineering, Chonnam National University, 300 Yongbong-Dong, Gwangju, 500-757, Republic of Korea

ARTICLE INFO

Article history:
Received 25 August 2008
Received in revised form 20 January 2009
Accepted 10 February 2009
Available online 13 February 2009

Keywords:
Free surface
Source
Sink
Stokes flow
Cusp
Surface tension
Capillary number
Conformal mapping

ABSTRACT

Two-dimensional Stokes flow due to a source and a sink of equal strength below the free surface is analyzed and free surface shape and cusp formation are discussed. The source-sink pair below the free surface are aligned vertical to the free surface. In the analysis, the Stokes' approximation is used and surface tension effects are included, but gravity is neglected. The solution is obtained by using conformal mapping and complex function theory. From the solution, typical free surface shapes are shown and formation of a cusp on the free surface is discussed. As the capillary number increases, the converging free surface shape becomes singular and tends to form a cusp for sufficiently large capillary number. Typically, streamline patterns for some capillary numbers are also shown. As the capillary number vanishes, the solution is reduced to the linearized potential flow solution.

1. Introduction

Since some flow visualizations by photographs of the cusp on the free-surface of both Newtonian and non-Newtonian fluids at low Reynolds numbers have been performed by Joseph [1], many theoretical and experimental researches are carried out [2,3]. These photographs show compelling evidence for the formation of two-dimensional sharp cusps on the free surface in the regions of converging flow. The dynamical mechanism related to this cusp singularity on the free surface in a Stokes flow has recently become an attractive subject of theoretical and experimental researches. The understanding of cusp formation is very important, since the presence of two-dimensional cusp on the free surface may result in a mechanism for air entrainment such as in chemical reaction or film coating. In the paper of Jeong and Moffatt [3], they carried out experiments using a pair of counter-rotating cylinders in a Newtonian fluid with free surface. For very slow rotation rates, there is a stagnation line on the free surface, and in some circumstances a small rounded crest can form in the neighborhood of this stagnation line. When the rotation rate is increased however, the surface dips downward, and simple visual observation indicates the presence of a very sharp cusp on the free surface. A complete analytical solution of a model problem of this experiments was also obtained, where the full nature of the flow and the detail of the cusp formation procedure were explained. In the model problem, they considered a Stokes flow induced by a vortex dipole below the otherwise undisturbed free surface, where direction of the vortex dipole was perpendicular to the free surface. Jeong [4] generalized this model problem to the case in which the orientation of the vortex dipole beneath the free surface is arbitrary. Antanovskii [5] generalized to the case in which the interfacial tension is variable, and Cummings [6] to the steady bubble solutions in dipole-driven Stokes flow. Jeong [7] also considered a Stokes flow induced by a single source or sink of arbitrary strength instead of a vortex dipole below the otherwise undisturbed free surface.

In this paper, we consider a Stokes flow due to a source and a sink of equal strength located below the free surface. The source-sink pair is aligned vertical to the free surface and the distance between the source and the sink is arbitrary. This flow is a generalized flow of Jeong and Moffatt [3] and Jeong [7], since these problems may be considered as the limit cases where the distance between the source and the sink approaches to zero and infinity, respectively. As a low Reynolds number limit, the Stokes' approximation is used and the effect of surface tension is included, but gravity effects are neglected. The solution is obtained analytically by using conformal mapping and complex function theory. From the solution, the deformation of the free surface and the formation of a cusp on the free surface are discussed and some streamline patterns are shown.

E-mail address: jtjeong@chonnam.ac.kr.

0997-7546/$ – see front matter
doi:10.1016/j.euromechflu.2009.02.003

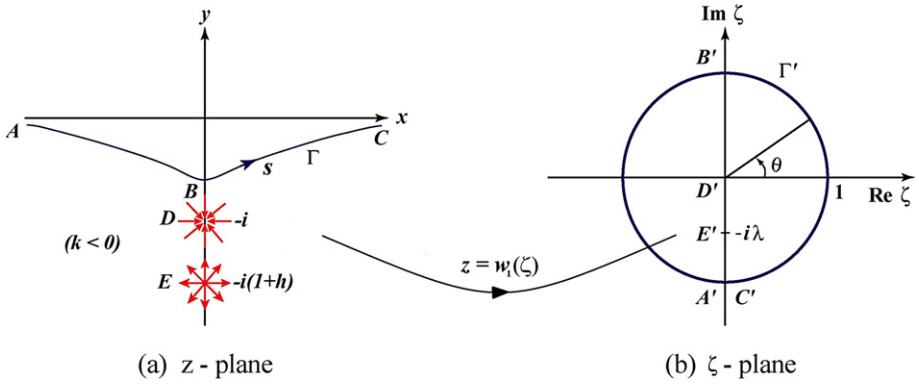

Fig. 1. Free surface deformation by a source-sink pair and conformal mapping from the flow field in z-plane into the inside of unit circle in ζ-plane.

2. The method of solution

2.1. Mathematical formulation

Consider the flow region shown in Fig. 1(a), where the undisturbed fluid occupies the half space $y < 0$. A line source of strength k (outward flowrate $2\pi k$) is located at $z(= x + iy) = -id$ and of strength $-k$ at $z = -id(1 + h)$. Source of negative strength may be considered as sink. To non-dimensionalize the length scale by d, we may take $d = 1$ in what follows and the source and the sink singularities are then located at $z = -i$ and $z = -i(1 + h)$, respectively. The flow is generated by this source-sink pair and the free surface Γ is distorted, while the free surface at far field should remain flat and the height of the free surface vanishes as $|x| \to \infty$.

Assume that the Reynolds number $Re \equiv k/\nu$ (ν: kinematic viscosity) is small so that the stream function Ψ satisfies the biharmonic equation $\nabla^4\Psi = 0$. It is well known that the stream function Ψ can then be expressed in the form [8]

$$\Psi = \mathrm{Im}\big[f(z) + \bar{z}g(z)\big], \tag{1}$$

where two complex functions $f(z)$, $g(z)$ are analytic at all points z in the fluid domain except at the source and sink singularities $z = -i$ and $z = -i(1 + h)$, i.e.,

$$f(z) \to k\ln(z + i) \quad \text{as } z \to -i, \tag{2}$$

$$f(z) \to -k\ln\big\{z + i(1 + h)\big\} \quad \text{as } z \to -i(1 + h). \tag{3}$$

The velocity components (u, v) are then given by

$$u - iv = f'(z) + \bar{z}g'(z) - \overline{g(z)}, \tag{4}$$

and the pressure (p) and vorticity (Ω) fields are given by

$$p - i\mu\Omega = 4\mu g'(z) \tag{5}$$

where μ is the viscosity. It is easy to verify that, with these relations, the Stokes equation $\nabla p = \mu\nabla^2\mathbf{u}$ is satisfied in the fluid.

As shown by Richardson [9], velocity and stress boundary conditions on the free surface Γ take the form

$$f'(z) + \bar{z}g'(z) - \overline{g(z)} = u_0(z)\overline{\left(\frac{dz}{ds}\right)}, \tag{6}$$

$$f'(z) + \bar{z}g'(z) + \overline{g(z)} = -i\frac{\gamma}{2\mu}\overline{\left(\frac{dz}{ds}\right)}, \tag{7}$$

where s is the arclength on Γ measured from the point of symmetry B (Fig. 1(a)), γ the surface tension coefficient, and $u_0(z)$ the (real) tangential velocity on the free surface. The manipulation of (6) and (7) yields the following equations (for $z \in \Gamma$);

$$f(z) + \bar{z}g(z) = 0, \tag{8}$$

$$\mathrm{Im}\left[\overline{\left(\frac{dz}{ds}\right)}g(z)\right] = \frac{\gamma}{4\mu}. \tag{9}$$

The conditions $u, v \to 0$ at infinity ($|z| \to \infty$) are satisfied provided

$$f(z) \to cz, \quad g(z) \to \bar{c}, \quad \text{as } |z| \to \infty, \tag{10}$$

where c is an arbitrary constant. We can find from (6) and (7) that the choice $c = -i\gamma/4\mu$ is appropriate. Eqs. (2), (3) and (6)–(10) constitute the essential boundary conditions that $f(z)$ and $g(z)$ must satisfy. The symmetry conditions $\Psi = 0$, $\Omega = 0$ on $x = 0$ clearly imply that

$$\mathrm{Im}\big\{f(iy)\big\} = 0, \qquad \mathrm{Re}\big\{g(iy)\big\} = 0. \tag{11}$$

Since this problem may be considered as a generalization of previous problems, [3,7] we follow the similar procedure as in Refs. [3] and [7].

2.2. Conformal mapping and solution procedure

Let $z = w_1(\zeta)$, yet unknown, be the conformal mapping that maps the fluid domain $\mathcal{D}$ onto the unit disk $\mathcal{D}'$: $|\zeta| \leqslant 1$. The points A, B, C, D, E of Fig. 1(a) map to the points A', B', C', D', E' of Fig. 1(b), respectively. Since the mapping places the (imaged) source and sink at $\zeta = 0$, $-i\lambda$ $(0 < \lambda < 1)$, respectively, the mapping function $w_1(\zeta)$ must satisfy,

$$w_1(0) = -i, \tag{12}$$

$$w_1(-i\lambda) = -i(1 + h). \tag{13}$$

If we set,

$$F(\zeta) \equiv f\big\{w_1(\zeta)\big\} = f(z), \tag{14}$$

$$G(\zeta) \equiv g\big\{w_1(\zeta)\big\} = g(z), \tag{15}$$

$$U(\zeta) \equiv u_0\big\{w_1(\zeta)\big\} = u_0(z), \tag{16}$$

then,

$$f'(z) = \frac{F'(\zeta)}{w_1'(\zeta)}, \qquad g'(z) = \frac{G'(\zeta)}{w_1'(\zeta)}. \tag{17}$$

By the conformal mapping properties, it follows that, for $z \in \Gamma$, i.e., $|\zeta| = 1$,

$$\frac{dz}{ds} = -i\zeta\frac{w_1'(\zeta)}{|w_1'(\zeta)|}, \tag{18}$$

$$\overline{\left(\frac{dz}{ds}\right)} = \frac{i}{\zeta}\frac{\overline{w_1'(\zeta)}}{|w_1'(\zeta)|}. \tag{19}$$

Hence, boundary conditions (6) and (7) become, on $|\zeta| = 1$,

$$\frac{F'(\zeta)}{w_1'(\zeta)} + \overline{w_1(\zeta)}\frac{G'(\zeta)}{w_1'(\zeta)} - \overline{G(\zeta)} = U(\zeta)\frac{i}{\zeta}\frac{\overline{w_1'(\zeta)}}{|w_1'(\zeta)|}, \tag{20}$$

and

$$\frac{F'(\zeta)}{w_1'(\zeta)} + \overline{w_1(\zeta)}\frac{G'(\zeta)}{w_1'(\zeta)} + \overline{G(\zeta)} = \frac{\gamma}{2\mu\zeta}\frac{\overline{w_1'(\zeta)}}{|w_1'(\zeta)|}. \tag{21}$$

Subtracting (20) from (21) and taking the complex conjugate gives

$$\frac{G(\zeta)}{\zeta w_1'(\zeta)} = \frac{1}{2|w_1'(\zeta)|}\left(\frac{\gamma}{2\mu} + iU(\zeta)\right), \quad \text{on } |\zeta| = 1. \tag{22}$$

Since $w_1(\zeta)$ is a conformal mapping function, $w_1'(\zeta)$ is analytic and non-zero in $|\zeta| < 1$, and the left-hand side of (22) is analytic in $|\zeta| < 1$ except a simple pole at $\zeta = 0$. To remove this singularity, we subtract $G(0)/\zeta w_1'(0)$ from each side of (22):

$$\frac{G(\zeta)}{\zeta w_1'(\zeta)} - \frac{G(0)}{\zeta w_1'(0)} = \frac{1}{2|w_1'(\zeta)|}\left(\frac{\gamma}{2\mu} + iU(\zeta)\right) - \frac{G(0)}{\zeta w_1'(0)} \quad \text{on } |\zeta| = 1. \tag{23}$$

Now, the left-hand side of (23) is the boundary value of a function analytic in $|\zeta| < 1$. If $w_1(\zeta)$ and $G(0)$ can be found, then the real part of the right-hand side of (23) will be known, so that $G(\zeta)$ may be found by using Cauchy's integral theorem [8]. Hence, the formal expression of $G(\zeta)$ is, for $|\zeta| \leqslant 1$,

$$\frac{G(\zeta)}{\zeta w_1'(\zeta)} = \frac{G(0)}{w_1'(0)}\left(\zeta + \frac{1}{\zeta}\right) + \frac{1}{2\pi i}\oint_{|\zeta_0|=1} \frac{\gamma}{4\mu|w_1'(\zeta_0)|}\frac{\zeta_0 + \zeta}{\zeta_0(\zeta_0 - \zeta)}\,d\zeta_0, \tag{24}$$

where $w_1'(\zeta)$ and $G(0)$ should be determined. To consider the behavior of this expression as $|\zeta| \to 1$, we put $\zeta_0 = e^{i\theta_0}$ and $\zeta = e^{i\theta}$ in (24), then

$$\frac{G(\zeta)}{\zeta w_1'(\zeta)} = 2\cos\theta\frac{G(0)}{w_1'(0)} + \frac{\gamma}{4\mu|w_1'(\zeta)|} + \frac{i\gamma}{8\pi\mu}\int_0^{2\pi}\frac{1}{|w_1'(e^{i\theta_0})|}\frac{\cos\theta + \cos\theta_0}{\sin\theta - \sin\theta_0}\,d\theta_0, \tag{25}$$

where the principal value is used for integral. Since $G(0)$ is pure imaginary from the symmetry condition (11) and $w_1'(0)$ must be real (see Fig. 1), it can be shown that the real part of this expression is $\gamma/4\mu|w_1'(\zeta)|$ as required by (22).

Now, consider that the boundary conditions (2), (3) are transformed in the ζ-plane as

$$F(\zeta) \to k\ln\zeta, \quad \text{as } \zeta \to 0, \tag{26}$$

$$F(\zeta) \to -k\ln(\zeta + i\lambda), \quad \text{as } \zeta \to -i\lambda, \tag{27}$$

respectively, where λ $(0 < \lambda < 1)$ is a real constant defined in (13). Moreover, the boundary condition (8) is transformed in ζ-plane as

$$F(\zeta) = -\overline{w_1(\zeta)}G(\zeta) = -w_1^*(\zeta)G(\zeta) \quad \text{on } |\zeta| = 1, \tag{28}$$

since $\bar{\zeta} = 1/\zeta$ on $|\zeta| = 1$. The conjugate function w_1^* in (28) is defined as $w_1^*(\zeta) = \overline{w_1(1/\bar{\zeta})}$. Note that the boundary conditions (26), (27) have logarithmic singularities at $\zeta = 0, -i\lambda$, which are somewhat difficult to be satisfied. However, considering bilinear transformation and observing the boundary conditions (26)–(28) carefully, we may construct an appropriate integral form of mapping function as

$$z = w_1(\zeta) = \frac{w(\zeta) - iJ}{J+1}, \tag{29a}$$

where

$$w(\zeta) = \int_0^{\lambda} ib(t)\frac{\zeta}{\zeta t + i}\,dt + i\frac{\zeta - i}{\zeta + i}, \tag{29b}$$

$$J = \int_0^{\lambda}\frac{b(t)}{t-1}\,dt, \tag{29c}$$

where a real constant λ $(0 < \lambda < 1)$ and a real function $b(t)$ in $0 \leqslant t \leqslant \lambda$ is to be determined. Since $w_1(0) = -i$ (12) is satisfied, and $\mathrm{Im}\{w_1(\zeta)\} \to 0$ as $\zeta \to -i$ on $|\zeta| = 1$, which implies the flat free surface as $|x| \to \infty$. Then the conjugate function $w_1^*(\zeta)$ can be written as

$$w_1^*(\zeta) \equiv \overline{w_1(1/\bar{\zeta})} = \frac{w^*(\zeta) + iJ}{(J+1)}, \tag{30a}$$

where

$$w^*(\zeta) = \overline{w(1/\bar{\zeta})} = -\int_0^{\lambda}\frac{ib(t)}{t - i\zeta}dt + i\frac{\zeta - i}{\zeta + i}. \tag{30b}$$

Note that the mapping function $w_1(\zeta)$ in (29) is analytic in $|\zeta| < 1$, whereas the conjugate function $w_1^*(\zeta)$ in (30) is analytic in $|\zeta| > 1$. By introducing $w_1(\zeta)$ of the form in (29), we may show that the logarithmically singular boundary conditions (26) and (27) can be satisfied. Substituting (30) into (28), we get $F(\zeta)$ in $|\zeta| \leqslant 1$, by applying Cauchy's integral theorem [8],

$$F(\zeta) = -w_1^*(\zeta)G(\zeta) = \frac{1}{J+1}\left\{\int_0^{\lambda}\frac{ib(t)}{t - i\zeta}\,dt - i\frac{\zeta - i}{\zeta + i} - iJ\right\}G(\zeta). \tag{31}$$

Since the stream function (1) must be discontinuous due to the source and sink of strength k, $F(\zeta)$ in (31) should have discontinuity $2\pi ik$ across the segment $D'E'$ in Fig. 1(b). Therefore,

$$G(-it_0) = \frac{ik(J+1)}{b(t_0)} \quad \text{for } 0 \leqslant t_0 \leqslant \lambda. \tag{32}$$

Substituting $\zeta = -it_0$ $(0 \leqslant t_0 \leqslant \lambda)$ in (24) and using (32), we get

$$-\frac{k(J+1)}{t_0 b(t_0) w'(-it_0)} = \frac{k(J+1)}{b(0)w'(0)}\left(t_0 - \frac{1}{t_0}\right) + \frac{1}{2\pi i}\oint_{|\zeta_0|=1}\frac{\gamma}{4\mu|w'(\zeta_0)|}\frac{\zeta_0 - it_0}{\zeta_0(\zeta_0 + it_0)}\,d\zeta_0, \tag{33}$$

where $w'(\zeta)$ the derivative of $w(\zeta)$ in (29b) is written as

$$w'(\zeta) = \frac{dw(\zeta)}{d\zeta} = -\int_0^{\lambda}\frac{b(t)}{(\zeta t + i)^2}\,dt - \frac{2}{(\zeta + i)^2}. \tag{34}$$

Now, when we compare the imaginary parts of (22) and (25), we obtain an expression for the tangential velocity on the free surface:

$$u_0(z) = U(\zeta) = U\left(e^{i\theta}\right) = -\cos\theta\left|w'\left(e^{i\theta}\right)\right| \times\left[\frac{4G(0)}{w'(0)}i + \frac{\gamma}{4\pi\mu}\int_0^{2\pi}\frac{d\theta_0}{|w'(e^{i\theta_0})|(\sin\theta_0 - \sin\theta)}\right]. \tag{35}$$

From the condition that $u_0(z) \to 0$ as $|z| \to \infty$ (i.e. as $\theta \to -\frac{\pi}{2}$ in (35)), the term in square bracket in (35) must vanish as $\theta \to -\frac{\pi}{2}$, i.e.

$$G(0) = \frac{ik(J+1)}{b(0)} = \frac{i\gamma w'(0)}{16\pi\mu}\int_0^{2\pi}\frac{d\theta_0}{|w'(e^{i\theta_0})|(\sin\theta_0 + 1)}. \tag{36}$$

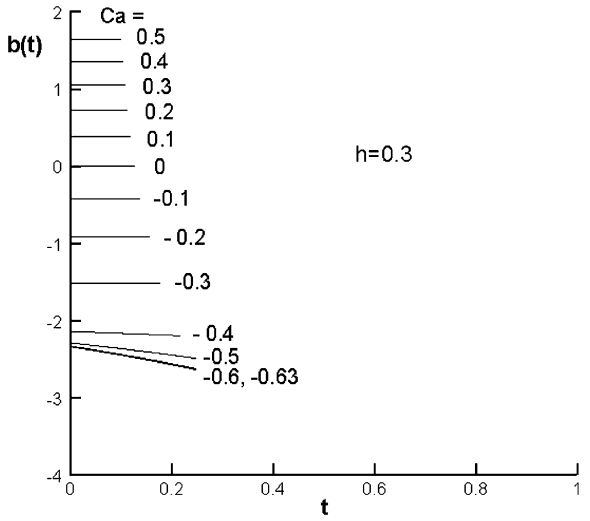

Fig. 2. Graphs of $b(t)$ $(0 \leqslant t \leqslant \lambda)$ in the mapping function $w_1(\zeta)$ of (29) for some capillary numbers Ca.

Combining (33), (36) and canceling $b(0)$, we obtain the relation as

$$\frac{1}{b(t_0)} = \frac{w'(-it_0)(1-t_0^2)(1-t_0)^2}{16\pi Ca(J+1)} \times \int_0^{2\pi} \frac{d\theta_0}{|w'(e^{i\theta_0})|(\sin\theta_0+1)(2t_0\sin\theta_0+1+t_0^2)}, \tag{37}$$

for $0 \leqslant t_0 < \lambda$, where the capillary number Ca is defined as

$$Ca \equiv \frac{\mu k}{\gamma d}. \tag{38}$$

Note that unknown λ and $b(t)$ $(0 \leqslant t \leqslant \lambda)$ are involved in J and w' of the right-hand side of (37) as shown in (29c) and (34). Eq. (37) together with (13) is a kind of non-linear integral equation [10] for real constant λ $(0 < \lambda < 1)$ and real function $b(t)$ $(0 \leqslant t \leqslant \lambda)$ with 2 given parameters h, Ca. Solving the integral equation (37) together with (13) numerically, we obtain λ and $b(t)$ $(0 \leqslant t \leqslant \lambda)$ for a given capillary number Ca and h. With λ and $b(t)$ obtained, we derive $G(\zeta)$ in $|\zeta| \leqslant 1$ from (24) and (36) as

$$G(\zeta) = -\frac{k}{32\pi Ca} w'(\zeta)\left(\zeta + \frac{1}{\zeta}\right)(\zeta+i)^2 I\big(\zeta; b(t)\big), \tag{39}$$

where

$$I\big(\zeta; b(t)\big) \equiv \int_0^{2\pi} \frac{d\theta_0}{|w'(e^{i\theta_0})|(1+\sin\theta_0)(\sin\theta_0 - (\zeta-\zeta^{-1})/(2i))}. \tag{40}$$

From (39), we can see

$$G(\zeta) \to i\gamma/4\mu \quad \text{as } \zeta \to -i,$$

which is consistent with boundary condition (10). Therefore, two complex functions $F(\zeta)$ and $G(\zeta)$ in the ζ-plane are obtained as (31) and (39), and hence $f(z)$ and $g(z)$ in the z-plane, which describe the whole solution of our flow due to the source-sink pair.

3. Results

To find λ and $b(t)$ for the given values of Ca and h, the non-linear integral equation (37) together with (13) is solved numerically. For the given value of Ca and initially assumed value of λ, the integral equation (37) is solved by using the iterative method. Then, h can be calculated from (13), which must be equal to the given value of h by adjusting the assumed value of λ. In the iterative method to solve the integral equation (37) for $b(t)$, we used the initial guess as $b(t) = 4Ca$ $(0 \leqslant t \leqslant \lambda)$ which is a solution for $Ca \to 0$. Graphs of $b(t)$ $(0 \leqslant t \leqslant \lambda)$ for some values of Ca are shown in Fig. 2 for $h = 0.3$ typically. Using λ, $b(t)$ determined in this way, we can show free surface shapes and streamline patterns for some values of capillary number Ca and dimensionless distance h.

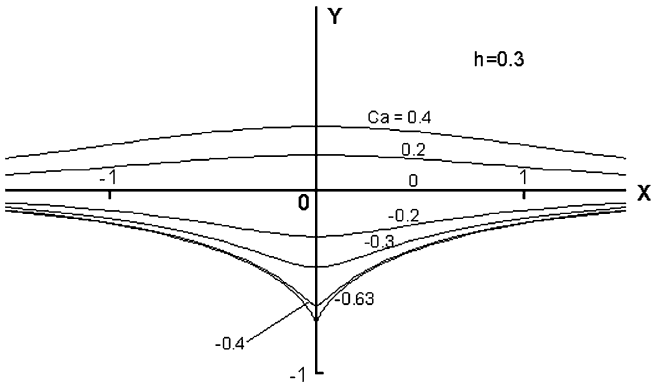

Fig. 3. Free surface shapes for some values of Ca.

3.1. Free surface

The free surface Γ is given by (29), i.e., $z = x + iy = w_1(\zeta)$ with $\zeta = e^{i\theta}$,

$$x(\theta) = \frac{\cos\theta}{J+1}\left\{\int_0^{\lambda} \frac{b(t)}{t^2+2t\sin\theta+1}\,dt + \frac{1}{1+\sin\theta}\right\}, \tag{41a}$$

$$y(\theta) = \frac{1}{J+1}\left\{\int_0^{\lambda} \frac{b(t)(t+\sin\theta)}{t^2+2t\sin\theta+1}\,dt - J\right\}. \tag{41b}$$

The free surface shapes are shown in Fig. 3 for some typical values of capillary number $Ca(=\mu k/\gamma d)$ when $h = 0.3$. As Ca decreases to -0.63, a cusp is likely to occur at the center $(x = 0)$ of the free surface. For the lower values of Ca, numerical calculation becomes hard to obtain a valid solution converged since the integrand in (37) becomes steep around $\theta_0 = \pi/2$. We may conjecture that as $Ca \to -\infty$, a genuine cusp would occur. In that case, $w'(i)$ approaches to zero and the mapping is not conformal at $\zeta = i$ so that the integral equation (37) becomes singular. Near the cusp point, as explained by Jeong and Moffatt [3] and Jeong [4], the characteristic length scale reaches to the molecular scale and the continuum hypothesis fails hence the effects of intermolecular forces should be considered. Eggers [11] insisted that the air (second fluid outside) drawn into the cusp entered the fluid destroying the cusp solution and the molecular scales were never reached.

From the limit $\theta \to -\frac{\pi}{2}$ in (41), we can see

$$y \to Cx^{-2} \quad \text{as } |x| \to \infty, \tag{42}$$

where

$$C = \frac{2}{(J+1)^3}\int_0^{\lambda} b(t)\frac{1+t}{(1-t)^3}\,dt.$$

In the limit of $Ca(=\mu k/\gamma) \to 0$, (37) is reduced to $b(t) \to 4(J+1)Ca$, hence $y = O(Ca)$ from (41b). This means that, for very large surface tension or very weak strength of source-sink pair, deformation of the free surface is very small and free surface shape tends to be horizontal. Moreover, from (41), we can obtain

$$y \approx 2Ca\ln\left(\frac{x^2+(1+h)^2}{x^2+1}\right), \quad \text{for } |Ca| \ll 1, \tag{43}$$

which agrees with a linearized result of our problem.

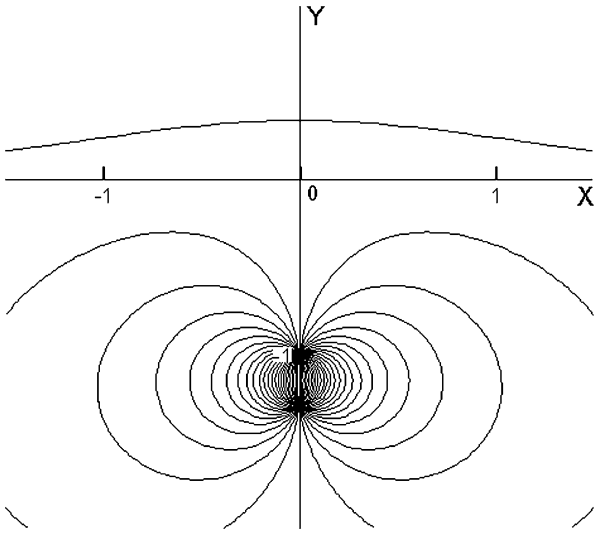

Fig. 4. Streamline pattern for $Ca = 0.4$ with $h = 0.3$. Here $\Delta\Psi/2\pi k = 0.02$.

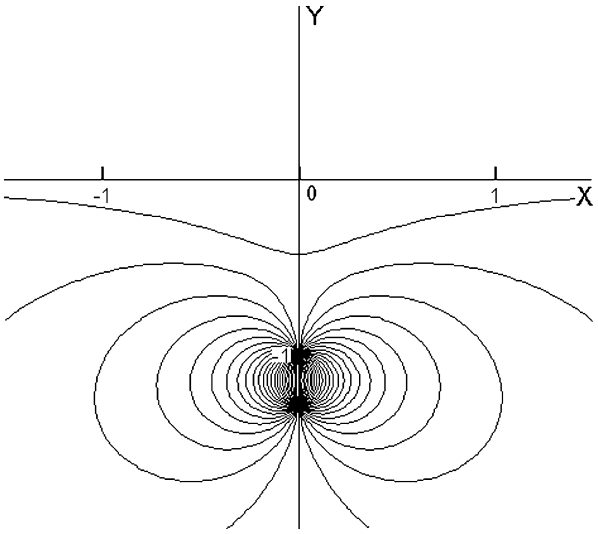

Fig. 6. Streamline pattern for $Ca = -0.3$ with $h = 0.3$. Here $\Delta\Psi/2\pi k = 0.02$.

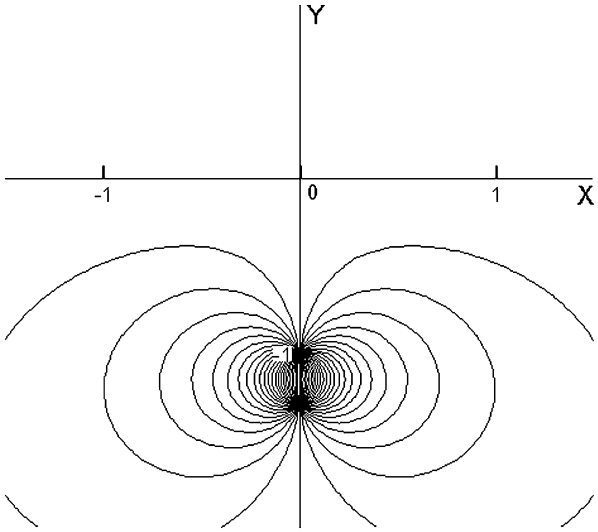

Fig. 5. Streamline pattern for $Ca = 0$ with $h = 0.3$. The results are exactly the potential flow solution. Here $\Delta\Psi/2\pi k = 0.02$.

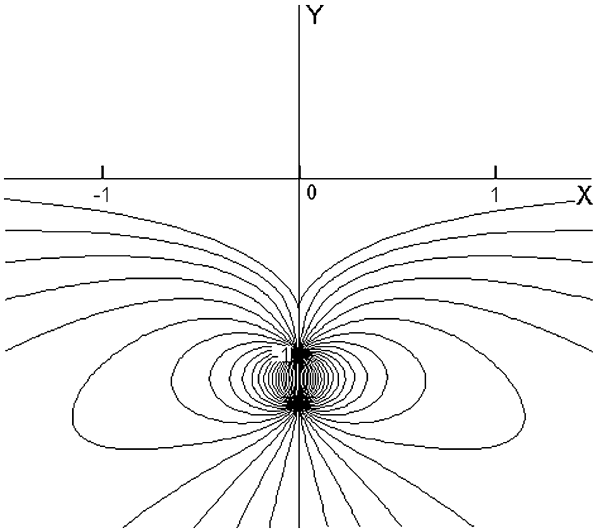

Fig. 7. Streamline pattern for $Ca = -0.63$ with $h = 0.3$. Here $\Delta\Psi/2\pi k = 0.02$.

3.2. Stream function and flow patterns

Substituting $F(\zeta), G(\zeta)$ obtained as (31), (39) into (1), we get a stream function as

$$\Psi = \frac{1-\zeta\bar{\zeta}}{J+1}\,\mathrm{Im}\left[G(\zeta)\left\{\int_0^{\lambda}\frac{b(t)}{(t-i\zeta)(\bar{\zeta}t-i)}\,dt+\frac{2i}{|\zeta+i|^2}\right\}\right]. \tag{44}$$

When $h = 0.3$, the streamline patterns for some typical values of $Ca = 0.4, 0, -0.3, -0.63$ are shown in Figs. 4–7.

Additionally, the tangential velocity $u_0(z)$ on the free surface Γ may also be derived from (35) with (36) as

$$\begin{aligned} u_0(z) &= U\left(e^{i\theta}\right) \\ &= -\frac{k}{4\pi Ca}(1+\sin\theta)\cos\theta\left|w'\left(e^{i\theta}\right)\right| \\ &\quad\times\left[\int_0^{2\pi}\frac{d\theta_0}{|w'(e^{i\theta_0})|(\sin\theta_0+1)(\sin\theta_0-\sin\theta)}\right], \end{aligned} \tag{45}$$

where the principal value is used for the integral. Since x is related to θ by (41a), Eq. (45) determines $u_0(\theta)$ as a function of $x(\theta)$ parametrically. The tangential velocity distribution is shown in Fig. 8 for some values of Ca. The curve corresponding to $Ca = 0$ coincides with that obtained by a linearized analysis. The free surface velocity is directed towards or away from the stagnation point on the free surface according as $Ca < 0$ or $Ca > 0$.

For the limiting case of the capillary number $Ca \to 0$,

$$w'(\zeta) \to \frac{-2}{(\zeta+i)^2}, \quad b(t) \to 4Ca, \quad G(\zeta) \to \frac{i\gamma}{4\mu}.$$

Hence the stream function Ψ in (44) becomes

$$\Psi \to -k\,\mathrm{Im}\left[\ln\left\{\frac{\zeta+i\lambda}{i\zeta(\lambda\bar{\zeta}-i)}\right\}\right] \to k\,\mathrm{Im}\left\{\ln\left(\frac{z^2+1}{z^2+(1+h)^2}\right)\right\},$$

and the tangential free-surface velocity $u_0(z)$ in (45) becomes

$$u_0(z) \to k\cos\theta\,\frac{2\lambda(1+\sin\theta)}{\lambda^2+1+2\lambda\sin\theta} \to \frac{2h(h+2)kx}{(x^2+1)\{x^2+(h+1)^2\}},$$

which agree well with the results of the linearized potential flow solution.

4. Conclusion

In this paper, Stokes flow due to a source-sink pair of arbitrary strength below the free surface is analyzed by using the complex

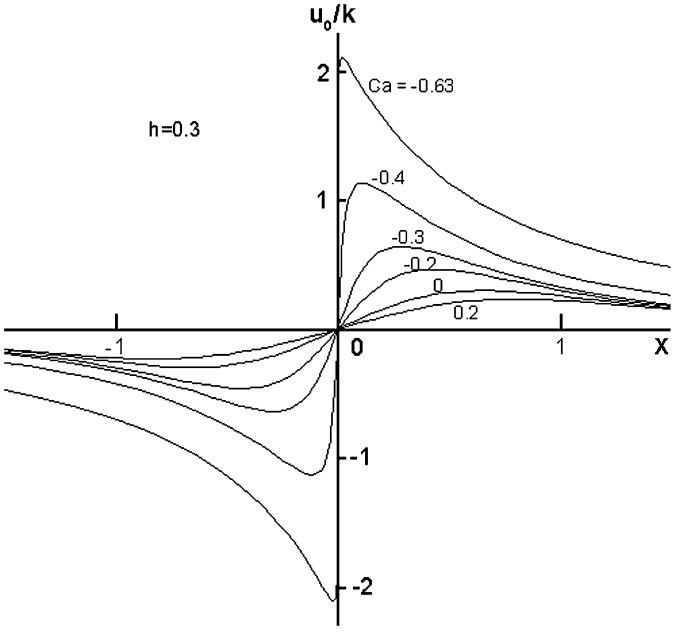

Fig. 8. Tangential velocity distribution $u_0(x)$ on the free surface Γ for some values of Ca.

function theory. While the gravity is neglected in this model, we have obtained many valuable insights into the formation of cusp on the free surface. Actually, near the cusp, surface tension effects are dominant to the gravitational effects. For arbitrary strength and distance of source-sink pair, the whole flow fields are determined including the free surface shape and the tangential velocity distribution on the free surface. We conclude that the cusp occurs on the converging free surface for sufficiently large capillary number Ca. As the capillary number vanishes, our solution tends to the well-known linearized potential flow solution, as expected. As the distance of source-sink pair $h \to 0$, the non-linear integral equation (37) reduces to $b(0) = 4Ca$. Here, if we maintain $kh =$ constant (dipole strength), it reduces to a non-linear equation and flow becomes that of Jeong and Moffatt. Much further theoretical research may also be motivated by considering the effects neglected in this analysis, such as air (second fluid outside) near the cusp, unsteadiness, variable surface tension, the gravity effects, and so on.

Acknowledgement

This study was financially supported by Chonnam National University, 2007.

References

[1] D.D. Joseph, J. Nelson, M. Renardy, Y. Renardy, Two-dimensional cusped interface, J. Fluid Mech. 223 (1991) 383.
[2] Y.J. Liu, T.Y. Liao, D.D. Joseph, A two dimensional cusp at the trailing edge of an air bubble rising in a viscoelastic liquid, J. Fluid Mech. 304 (1995) 321.
[3] J.-T. Jeong, H.K. Moffatt, Free-surface cusps associated with flow at low Reynolds number, J. Fluid Mech. 241 (1992) 1.
[4] J.-T. Jeong, Formation of cusp on the free surface at low Reynolds number flow, Phys. Fluids 11 (1999) 521.
[5] L.K. Antanovskii, Influence of surfactants on a creeping free boundary flow induced by two counter-rotating horizontal thin cylinders, Eur. J. Mech. B/Fluids 13 (1994) 73.
[6] L.J. Cummings, Steady solutions for bubbles in dipole-driven Stokes flows, Phys. Fluids 12 (2000) 2162.
[7] J.-T. Jeong, Free surface deformation due to a source or a sink in Stokes flow, Eur. J. Mech. B/Fluids 26 (2007) 720.
[8] N.I. Muskhelishvili, Some Basic Problems of the Mathematical Theory of Elasticity, third ed., P. Noordhoff, 1953.
[9] S. Richardson, Two dimensional bubbles in slow viscous flows, J. Fluid Mech. 33 (1968) 475.
[10] F.G. Tricomi, Integral Equations, fourth ed., John Wiley & Sons, Inc., 1967, pp. 197–213.
[11] J. Eggers, Air entrainment through free-surface cusp, Phys. Rev. Lett. 86 (2001) 4290.